paper no. 55—SA-58

The American Society of Mechanical Engineers

29 WEST 39TH STREET, NEW YORK 18, NEW YORK

THE FLOW IN A VEE-GUTTER CASCADE

W. G. Cornell, Member ASME
Aerodynamicist
General Electric Company
Aircraft Gas Turbine Division
Cincinnati, Ohio

Contributed by the Aviation Division and the American Rocket Society for presentation at the ASME Diamond Jubilee Semi-Annual Meeting, Boston, Mass. - June 19-23, 1955. (Manuscript received at ASME Headquarters April 25, 1955).

Written discussion on this paper will be accepted up to July 26, 1955.

(Copies will be available until April 1, 1956)

ABSTRACT

A theory is presented, yielding the wake shape, the total pressure loss, and the drag force of two-dimensional vee-gutter profiles in unstaggered cascade array, for incompressible, steady, potential flow directed normal to the cascade axis. The results, for all gutter-included angle and blockage ratio, are compared to two- and three-dimensional experimental results, showing good argreement. Approximate theories are presented, valid at high blockage ratio and either at small or large gutter angle.

1650-55

THE FLOW IN A VEE-GUTTER CASCADE

By W. G. Cornell

NOMENCLATURE

The following nomenclature is used in the paper:

A_q = function in expression for μ

B_q = function in expression for μ

b = breadth of gutter along cascade axis

C_C = contraction coefficient

C_D = drag coefficient

D = drag force on a gutter

d_1, d_2 = inlet, outlet diameter of conical nozzle

$F(b/t, \alpha)$ = function in expression for μ

$G(\alpha)$ = function in asymptotic expression for μ

$H(\alpha)$ = function in asymptotic expression for μ

p = static pressure

P_T = total pressure

Δp_T = total pressure loss of cascade

q = integer

R, Z = cylindrical coordinates

r, s = integers ($r > s$)

t = pitch of cascade along cascade axis

$W = \phi + i\psi$ = complex potential

w = fluid velocity

w_1 = velocity upstream of cascade

w_2 = velocity downstream of cascade

w_3 = velocity after mixing of wakes and jets

Y, X = rectangular co-ordinates

$z = x + iy$ = complex position variable

α = gutter included half-angle

β_q = function in expression for μ

ϵ = function in expression for μ

ζ = complex position variable

λ = total pressure loss coefficient of cascade

μ = wake width as fraction of pitch t

ξ = dummy variable of integration

ρ = fluid-mass density

INTRODUCTION

In afterburners of modern aircraft gas-turbine power plants and in other combustion systems, various bluff bodies are used for flameholders, creating low-velocity regions downstream in order to stabilize combustion. One of the most frequently used configurations is the vee-gutter flameholder, composed of concentric annular rings of vee cross section with apex upstream. In the design of vee-gutter flameholders, a method is needed to predict the effect of vee-gutter geometry on aerodynamic forces on the gutters, total pressure loss and wake shape.

The present theory idealizes the configuration as a two-dimensional cascade of vee-gutter profiles, that is, an infinite number of equally spaced profiles of infinite span, a section normal to the span being shown in Fig. 1. The profiles are idealized as infinitesimally thin vee-shaped plates of included angle 2α and breadth b along the cascade axis which is normal to the upstream flow.

The upstream flow, infinitely far ahead of the cascade, at station 1, is taken as a uniform flow of velocity w_1 normal to the cascade axis. Stagnation streamlines will proceed undeflected from station 1 to stagnation points at S on the apex of each profile. These streamlines then split and become the outside surfaces of the profiles, flowing smoothly off the trailing edges T. Since in an actual, viscous fluid, the flow cannot negotiate the sharp turn at the trailing edges in order to proceed upstream along the inside surfaces of the profiles, it will be assumed that the flow separates from the profile at the trailing edges. The streamlines extending downstream from the trailing edges will be taken as "free streamlines," enclosing "dead water" regions or wakes, extending infinitely far downstream to station 2. At station 2 the flow consists of wakes of extent μt parallel to the cascade axis, and intervening jets of extent $(1 - \mu)t$. In the wakes, the velocity is taken as zero, in the jets at a constant value w_2, normal to the cascade axis. The static pressure will be considered uniform across both wakes and jets at station 2. Thus, the static pressure in the entire wakes will be taken

constant at the downstream value p_2. As a boundary condition, then, the static pressure will be constant at p_2 along the free streamlines.

It will be assumed that the flow is two-dimensional, steady, incompressible, irrotational, nonviscous, and free of body forces. As a consequence, the velocity w_2 in the jets will exceed the inlet velocity w_1. Further, the total pressure $p_T = p + 1/2(\rho w^2)$ will be constant in the flow from 1 to 2, so that no losses will be accounted for in the process of formation of the jets.

The wakes and jets are then assumed to mix at constant momentum, since no mechanism is present to afford a force external to the fluid, between station 2 and station 3, located farther downstream. The flow at station 3 is characterized by uniform velocity w_3 normal to the cascade axis and equal, from continuity considerations, to the inlet velocity w_1. The static pressure will be taken as uniform at p_3, a lower value than the inlet static pressure p_1, since a total pressure loss will be computed in the mixing.

The problem may be stated as follows: Given a vee-gutter cascade defined geometrically by α, b/t and an upstream flow velocity w_1, it is required to find the wake thickness/pitch ratio μ, the drag force D (normal to the cascade axis) on each profile and the total pressure loss $\Delta p_T = p_{T1} - p_{T3}$.

FLOW IN THE WAKES AND JETS

The flow between stations 1 and 2 is considered first. The vee-gutter flow configuration shown in Fig. 1 is seen to be identical, under the assumptions made, to the configuration shown in Fig. 2, that of flow in a two-dimensional contraction, formed of two semi-infinite walls RS and extensions ST inclined at angle α to RS and having breadth b/2 measured normal to RS. At station 1, infinitely far ahead of the contraction, the velocity is w_1. The flow discharges into stagnant fluid having static pressure p_2 and forms a vena contracta of breadth $(1 - \mu)t$ at station 2, infinitely far downstream. Von Mises (1)[1] has given the desired potential-flow solution for the two-dimensional contraction, in order to predict flow coefficients for discharge from such openings, utilizing the free streamline theory of Helmholtz and Kirchoff (2). The results, in the present nomenclature, are as follows: The wake thickness/pitch ratio μ is given by

$$\mu = 1 - \frac{1 - b/t}{1 + F(\alpha, b/t)} \quad . \quad . \quad . \quad . \quad . \quad . \quad (1)$$

where

$$F(\alpha, b/t) = \frac{\sin \alpha}{\pi} \sum_{q=1}^{\frac{1}{2}r} \left\{ A_q \cos (s\beta_q) + B_q \sin (s\beta_q) \right\}$$

---

[1] Underlined numbers in parentheses refer to the Bibliography at the end of the paper.

r, s = arbitrary integers, $r > s$, $r/s = \pi/\alpha$

$$\beta_q = (2q - 1)\ \alpha/s$$

$$A_q = 2 \ln (1 - \cos \beta_q) +$$
$$- (\epsilon - 1/\epsilon) \ln (\epsilon^{2/s} - 1 - 2\epsilon^{1/s} \cos \beta_q)$$

$$B_q = 2(1/\epsilon - \epsilon)\ tg^{-1}\left\{\frac{\epsilon^{1/s} \sin \beta_q}{1 - \epsilon^{1/s} \cos \beta_q}\right\}$$

$$\epsilon = (1 - \mu)$$

In order to evaluate $F(\alpha, b/t)$ for chosen α, b/t, the integers r, s are chosen to yield the minimum number of series terms. It is to be noted that computation is restricted to values of α which are integral fractions of π. This restriction is not troublesome, however, since graphical interpolation can be used on the results. Numerical results are shown in Figs. 3 and 4, where μ is shown as a function of α and b/t for the complete range $0 < \alpha < 180^\circ$, $0 < b/t < 1$. Also shown in Fig. 3 are results of two asymptotic theories discussed later in the paper.

TOTAL PRESSURE LOSS

The total pressure loss $\Delta p_T = p_{T1} - p_{T3}$ may be written as

$$\Delta p_T = p_2 - p_3 + \tfrac{1}{2}\rho\,(w_2^2 - w_3^2) \quad . \quad . \quad . \quad . \quad (2)$$

by definition of $p_T = p + (1/2)\ \rho w^2$ and since $p_{T1} = p_{T2}$.

The principle of conservation of momentum may be applied for forces normal to the cascade axis and acting on a strip of fluid of breadth t, containing a wake and two halves of a jet, extending between stations 2 and 3. The result is

$$p_2 - p_3 = \rho\left\{w_3^2 - w_2^2\,(1 - \mu)\right\} \quad . \quad . \quad . \quad . \quad . \quad (3)$$

The principle of conservation of mass may be applied to the same strip, extended to station 1, to yield

$$w_1/w_2 = w_3/w_2 = 1 - \mu \quad . \quad . \quad . \quad . \quad . \quad . \quad (4)$$

Combination of Equations (2), (3), and (4) yields the nondimensional total pressure-loss coefficient as

$$\lambda \equiv 2\Delta p_T/\rho w_1^2 = \mu^2/(1-\mu)^2 \quad . \quad . \quad . \quad . \quad (5)$$

The loss coefficient λ is seen to be a function only of μ, which is given by Equation (1) in terms of α, b/t. Numerical results are shown in Figs. 5 and 6, where λ is shown as a function of α and b/t. Also shown in Fig. 5 are the results of the asymptotic theories.

PROFILE DRAG FORCE

The principle of conservation of momentum may be applied to the previous strip of fluid, extended to station 1, to yield the drag force on a profile as

$$D = (p_1 - p_2)t + \rho w_1^2 t - \rho w_2^2 t(1-\mu) \quad . \quad . \quad . \quad .(6)$$

Since the total pressure is unchanged between stations 1 and 2, the Bernoulli relation yields

$$p_1 - p_2 = \tfrac{1}{2}\rho(w_2^2 - w_1^2) \quad . \quad . \quad . \quad . \quad . \quad . \quad (7)$$

Combining Equations (4), (6), and (7) yields the nondimensional drag coefficient as

$$C_D \equiv D/(1/2)\rho w_1^2 b = (t/b)\mu^2/(1-\mu)^2 \quad . \quad . \quad . \quad . \quad (8)$$

which, with Equation (5), may be written as

$$C_D = (t/b)\,\lambda \quad . \quad . \quad . \quad . \quad . \quad . \quad . \quad (9)$$

which might have been deduced physically. The drag coefficient C_D is seen to be a function only of μ, or alternately of λ, and therefore of α and b/t from Equation (1). Numerical results are shown in Figs. 7 and 8, where C_D is shown as a function of α and b/t. The drag coefficient for the case of a single vee-gutter,

$b/t = 0$, has been given previously by Bobyleff(3). Also shown in Fig. 7 are the results of the asymptotic theories.

PHYSICAL SIGNIFICANCE OF THE RESULTS

The important physical results are shown in Fig. 5 through 8. The wake width/pitch ratio μ, the total pressure loss coefficient λ, and the drag coefficient C_D are seen to increase with blockage ratio b/t as expected physically. Similarly, they are seen to increase with gutter half-angle α, with a decreasing rate as α is increased from $\alpha = 0$ to $\alpha = 180^\circ$. The wake width, loss and drag at $\alpha = 90$ deg are considerably higher than those at $\alpha = 0$. However, the values at $\alpha = 180$ deg are only slightly higher than those at $\alpha = 90$ deg.

Some explanation of the limiting geometries is in order. At constant blockage b/t, the case of $\alpha = 0$ corresponds to a gutter made up of two coincident sides parallel to the upstream flow direction, with "open" end downstream. Thus, the breadth $b = 0$ and for $b/t \neq 0$, the pitch $t = 0$. Thus, $\mu > 0$ still implies wake width $\mu t = 0$. The loss coefficient $\lambda > 0$, but $\Delta p_T = 0$, $w_1 = 0$ since the space is "full of gutters." At constant blockage b/t, the case of $\alpha = 180$ deg corresponds to the same gutter as for $\alpha = 0$, but with "open" end upstream. In this case, an impediment to the flow is present in that the fluid must flow in and then back out of the rectangular channel of breadth $b = 0$. Again, the pitch $t = 0$ for constant $b/t \neq 0$, and $\mu > 0$ implies wake width $\mu t = 0$. Again $\lambda > 0$, $\Delta p_T = 0$, $w_1 = 0$. The case of blockage $b/t = 0$ is that of a single gutter, since $b > 0$ and $t = \infty$. In this case, $\mu = 0$ since $t = \infty$, $\lambda = 0$ since $w_1 > 0$, and $C_D > 0$. The case of blockage $b/t = 1.0$ is that of zero gap $t - b$ between adjacent plates. In this case $\mu = 1.0$ (downstream space filled with wakes), $\lambda = \infty$ and $C_D = \infty$ since $w_1 = 0$.

The effect of compressibility has been ignored for simplicity of analysis. Luckily, in modern afterburner practice Mach numbers are low (order of 0.1 - 0.2), so that the incompressible approximation is probably reasonable. At higher Mach numbers, additional losses may be expected. The effect of fluid friction is neglected, and thereby all consideration of scale effects. The theory should be most valid for high Reynolds numbers; i.e., for large gutters in high-velocity, high-density, low-viscosity fluids. At low Reynolds number, the actual wake width parameter μ will be larger than the theory predicts, leading to higher loss and drag. This follows from knowledge of the fact that nozzle flow coefficients decrease with Reynolds number and that the "flow coefficient" of the vee-gutter is proportional to $1 - \mu$.

The theoretical shape of the free streamlines could be calculated from the theory. However, weighting the analytical complexity of such a calculation against the practical value of the results leads one to be satisfied with the above statement. For estimation purposes, a reasonable wake boundary can be sketched, using the computed wake width μt and the boundary condition that the free streamlines are tangent to the gutter trailing edges.

THE ASYMPTOTIC THEORIES

Owing to the analytic complexity of the exact theory, it is convenient to have simpler results, approximately valid over part of the range of variables. Weinig (4) gives an asymptotic theory, valid for small α and large b/t, based upon

an analysis entirely similar to that of the exact theory. In place of the von Mises solution, Weinig uses his own asymptotic solution (5) of the potential flow problem of discharge from a two-dimensional contraction, for the case $\alpha \to 0$, $b/t \to 1$. Weinig's results are as follows:

$$\mu \sim 1 - \frac{1 - b/t}{1 + G(\alpha)} \quad . \quad . \quad . \quad . \quad . \quad . \quad (10)$$

where

$$G(\alpha) \equiv \frac{4}{\pi^2} \alpha \left\{ 1 + 0.085 \left(1 - \frac{2\alpha}{\pi} \right)^2 \right\}$$

The fundamental relations Equations (5) and (9) for $\lambda(\mu)$ and $C_D(\lambda)$ still obtain. Comparison of Equations (1) and (10) shows the same general form of $\mu(b/t, \alpha)$ in the exact and asymptotic theories, with the approximation $F(b/t, \alpha) \sim G(\alpha)$ for small α and large b/t. In Figs. 3, 5, and 7, the Weinig asymptotic theory is compared to the exact theory. It is seen that the asymptotic theory gives good results, μ, λ, and C_D being higher than the exact values, for the case of small α and large b/t.

A second asymptotic theory can be developed for the case of large α and large b/t. Weinig (6) has shown that a "bell mouth," suitable for an inlet in a turbomachine test stand, can be designed for constant velocity on the surface. Potential theory methods (2) are applied as follows: The desired bell mouth flow in the z-plane is describable in terms of an unknown complex potential $W = \phi + i\Psi$. The z-plane is mapped conformally on the ζ-plane, containing as image of the bell mouth flow a uniform flow,[2] given by $W = -\zeta$. Physical deduction shows that $\ln(dW/dz) = -e^{-i\pi}$ is a reasonable, yet simple expression for the ζ-plane image of the isotach-isocline field of the z-plane. Then, having $dW/d\zeta$ and dW/dz in terms of ζ, the derivative $dz/d\zeta$ of the transformation function is obtained. Integration yields $z = -Ei(e^{\zeta})$, where $-Ei(-x) \equiv \int_x^{\infty} (e^{-\xi}/\xi) d\xi$ is the exponential integral and ξ is a dummy variable of integration. Further investigation shows that the bell-mouth contour is the Sici spiral shown in Fig. 9, where $z = x + iy$ and:

$$\left.\begin{aligned} \frac{2x}{\pi} &= \frac{2}{\pi} \left(Ci(\alpha) \right. \\ \frac{2y}{\pi} &= 1 + \frac{2}{\pi} Si(\alpha) \end{aligned}\right\} \quad . \quad . \quad . \quad . \quad . \quad . \quad (11)$$

---

[2] Taking velocity proportional to the positive potential derivative.

and $Ci(\alpha) \equiv -\int_{\alpha}^{\infty}(\cos\alpha/\alpha)\,d\alpha$ and $Si(\alpha) \equiv (\pi/2) - \int_{\alpha}^{\infty}(\sin\alpha/\alpha)\,d\alpha$ are respectively the cosine and sine integrals.

The angle α is the local inclination of the bell-mouth contour. The potential flow pattern of the bell mouth can be applied to the vee-gutter configuration as shown in Fig. 10. At chosen points P on the bell-mouth contour, the upstream flow is taken as that off the trailing edges of vee-gutters in a cascade of large blockage b/t and half-angle α. The downstream portions of the bell-mouth contour are taken as the free streamlines of the vee-gutter cascade. The wake width parameter μ is then given by

$$\mu \sim 1 - \frac{1 - b/t}{1 + H(\alpha)} \quad . \quad . \quad . \quad . \quad . \quad (12)$$

where

$$H(\alpha) \equiv \frac{2}{\pi} Si(\alpha)$$

Again, Equations (5) and (9) give $\lambda(\mu)$ and $C_D(\lambda)$. The same general form of $\mu(b/t, \alpha)$ is obtained as in Equations (1) and (10), with the approximation that $F(b/t, \alpha) \sim H(\alpha)$ for large α and large b/t. In Figs. 3, 5, and 7, the present asymptotic theory is compared to the exact theory. The asymptotic theory gives fairly good results, the range of validity being restricted to very large α and b/t, and μ, λ, and C_D being higher than the exact values.

COMPARISON WITH EXPERIMENTAL RESULTS

Noreen (7) tested single vee-gutters of 90 deg included angle ($\alpha = 45^{\circ}$) and various widths b in a rectangular channel (span = 2 in., wall spacing t = 4 in.). The blockage ratios b/t were 0.5, 0.625, 0.75. Tests were made with air at velocities from 25 to 90 fps and with and without combustion. Pressure drop across the vee-gutter section was determined by measurement of wall static pressure before and behind the vee-gutter. In Fig. 11 are shown test values of loss coefficient λ plotted as a function of b/t, compared with the theoretical curve for $\alpha = 45$ deg. Measured losses with combustion exceed those predicted theoretically. Measured losses without combustion are less than theory predicts. The undoubtedly imperfectly square edges of the vee-gutter trailing edges probably are partially responsible for the relatively low loss of the cold tests. Thus, the theory assumes that the wake leaves tangent to the vee-gutter surface at the trailing edge. If the edge is slightly rounded, the flow will follow the contour, leading to a thinner wake, and, hence, lower loss.

In the case of the hot tests, additional losses occur due to heat addition. The disparity between theory and experiment is least at high blockage b/t, becoming higher as b/t is decreased. This is to be expected, since the theory's assumption of wake-pressure constant at the downstream value becomes less valid as blockage is decreased. In the case of low blockage cascades, the actual wake pressure is

somewhat below the downstream value, giving rise to relatively high drag, thick wake, and large loss compared to the theoretical value. As blockage is increased, strong accelerations are forced in the flow from inlet to jets between the wakes, and the theoretical assumption is more nearly representative of fact.

Noreen (7) also made spark Schlieren photographs of the wake flow. In general, the wake boundaries tended to roll up into vortices and ultimately to become turbulent. Examination of the photographs showed that the theoretical wake boundary lay approximately along an eye estimate of the locus of the centers of the rolled-up vortices. Typical photographs are shown in Fig. 12. In the photographs, the flow proceeds from right to left. The upper trailing edge of the vee-gutter is seen, and the light field is the field of flow. The vertical marks at the top of the photographs were 1 in. apart on the model. Shown on the photographs are the theoretical wake boundary, as well as the "effective" wake boundary computed from the measured loss coefficient. The theoretical wake is thinner than the "effective" wake in the hot tests, the converse being true in the cold tests.

Test data of Grey and Wilsted (8) are shown, compared with theory, in Figs. 13 and 14. Tests were made in air with axi-symmetrical conical nozzles of various cone angle and diameter ratio. The original data were presented in the form of curves of contraction coefficient as a function of cone angle, diameter ratio, and nozzle pressure ratio. For comparison with the present vee-gutter theory, the original data were extrapolated to zero pressure ratio and reworked into the form of wake-width parameter μ as a function of gutter half-angle α and blockage b/t, for the equivalent two-dimensional case, defined as that one having the same fraction of blocked area as the three-dimensional case of the experiment. Thus, with d_1 and d_2, respectively, the inlet and outlet diameters of the conical nozzle, the blockage ratio of the equivalent vee-gutter is given by

$$\left(\frac{b}{t}\right)_{eq.} = 1 - \left(\frac{d_2}{d_1}\right)^2 \quad . \quad . \quad . \quad . \quad . \quad . \quad (13)$$

The contraction coefficient is related to μ and b/t by

$$C_C = \frac{1 - \mu}{1 - \frac{b}{t}} \quad . \quad . \quad . \quad . \quad . \quad . \quad (14)$$

from the geometry of the configuration shown in Fig. 1.

The validity of this comparison of two- and three-dimensional flows is well known. The classical example is the fact that the theoretical contraction coefficient for a two-dimensional sharp-edged orifice (long slit) is very nearly equal to the experimental value for circular sharp-edged orifices (2). Other examples are cited by Weinig (9), the writer (10), and given later. The limitations of the validity of such comparisons of two- and three-dimensional flows

are principally governed by the following consideration. If a three-dimensional flow with radial co-ordinate denoted by R and axial co-ordinate by Z be compared with a two-dimensional flow with "comparable" co-ordinates denoted by Y and X, then a comparison such as that discussed is based upon the following imputed co-ordinate transformation

$$\left.\begin{aligned} X &= Z \\ Y &= R^2 \end{aligned}\right\} \quad . \quad . \quad . \quad . \quad . \quad . \quad (15)$$

Consideration of the nonlinear nature of the Y, R relation quickly indicates that the comparison is valid only for flows in which the radial (R) components of velocity are relatively small. In cases where large radial velocities exist, a vee-gutter in the three-dimensional R, Z -space transforms into a gutter of curved elements in the two-dimensional Y, X -space. Only for the cases of small radial velocity does a vee-gutter in R, Z become (approximately) a vee-gutter in Y, X. Thus, in the vee-gutter case, for gutters of small half angle α, the comparison is most valid. Further, for large blockage (and, hence, small velocity along the cascade axis) most validity is found. Examination of Fig. 13 shows good agreement between theory and experiment. Best agreement is noted at high blockage b/t, as expected, and at high gutter half-angle α. This latter is unexpected from the foregoing considerations. However, a further factor probably is responsible for overriding this: At high gutter angle, the "effective blockage" is greater and more acceleration is forced upon the jets between the wakes, leading to more accurate theoretical prediction (similarly to the effect discussed previously under the effect of blockage b/t). Fig. 14 shows theory and experiment for the case of $\alpha = 90$ deg, wake-width parameter μ being shown as a function of blockage b/t. Good agreement is obtained.

The data of Betz and Petersohn (11) on two-dimensional cascades of sharp-edged flat plates—equivalent to the case of $\alpha = 90$ deg—are also shown on Fig. 14. Tests were made with air and also with water discharging into atmospheric air. The velocity in the jets between the wakes was reported, calculated from static pressure measurements downstream of the cascade. In the present comparisons, wake width parameter μ was calculated from $tw_1 = (1 - \mu)tw_2$, the continuity relation, using experimental values of w_1/w_2. It is noted that the experimental vaues of μ are less than those predicted theoretically, an effect no doubt partially due to imperfect sharpness of plate edges.

Figs. 15, 16, and 17 show test results of Langer (12), who measured forces with a two-component balance on cascades of the profiles shown corresponding to vee-gutters of half-angle $\alpha = 90$, 140.5, 180 deg and to various blockages b/t. The data are shown as normal force coefficient $C_D(w_1/w_2)^2$, or drag coefficient based on jet velocity w_2, as a function of blockage b/t. It is noted that at low blockage b/t experimental drag coefficient is generally less than that predicted theoretically, an unexpected result. However, agreement improves with increasing blockage, as expected. At high blockage, experimental drag coefficients exceed theoretical values as expected.

Experimental data of Flachsbart (13) are shown on Fig. 18, compared with the theory. The data are shown as total pressure loss coefficient λ as a function of blockage b/t, for tests with air in three-dimensional screens formed of rectangularly-woven thin sheet metal strips, with flow normal to the plane of the screen. The original three-dimensional data have been converted to equivalent two-dimensional data on the basis of equal blocked area ratio, as previously discussed. Good agreement is noted between theory and experiment, measured losses being lower, probably due to slight rounding of the plate edges. This comparison of theory and experiment was first noted by Weinig (9) in his study of ribbon parachutes.

CONCLUSION

The present theory gives a reasonable means of predicting the performance of high blockage cascades of vee-gutter profiles, yielding the wake shape, the total pressure loss and the drag force on the profiles. Consequently, the effects of design choice of blockage and gutter angle can be predicted prior to proof testing of after burner flameholders of vee-gutter type.

ACKNOWLEDGMENTS

The author is indebted to Dr. F. S. Weinig for many suggestions, to Mr. A. E. Noreen for obtaining the experimental data of reference (7), and to Messrs. H. A. Fremont, J. E. Worsham and J. W. Vdoviak for many halpful discussions and references to combustion literature.

BIBLIOGRAPHY

1 "Berechnung von Ausfluss - und Ueberfallizahlen," by R. von Mises, Zeitschrift des Vereines deutscher Ingenieure, bd. 61, no. 21, pp. 447-452; no. 22, pp. 469-474; no. 23, 1917, pp. 493-498.

2 "Hydrodyanmics," by H. Lamb, Dover Publications, New York, N.Y., 6th ed., 1945.

3 By D. Bobyleff, Journal of the Russian Physico-Chemical Society, vol. 13, 1881.

4 Unpublished, by F. S. Weinig, 1951.

5 "Ausfluss aud einer Duese," by F. S. Weinig, Ingenieur-Archiv, bd. 11, 1940, pp. 264-268.

6 Unpublished, by F. S. Weinig, 1952.

7 Unpublished, by A. E. Noreen, 1954.

8 "Performance of Conical Jet Nozzles in Terms of Flow and Velocity Coefficients," by R. E. Gray and H. D. Wilsted, NACA Technical Note, No. 1757, November, 1948.

9 "Parachutes with Canopies Composed of Self-Supporting Ribbons," by F. V. Weinig, HQAMC, Wright Field, Technical Report No. F-TR-2148-ND, GS-AAF-Wright Field No. 22, 1947, pp. 13-14.

10 "The Stall Performance of Cascades," by W. G. Cornell, Proceedings of the 2nd U. S. National Congress of Applied Mechanics, Ann Arbor, Mich., 1954.

11 "Anwendung der Theorie der Freien Strahlen," by A. Betz and E. Petersohn, Ingenieur-Archiv, bd. 2, 1931, pp. 190-211.

12 "Bremswirkung von Windschutzgittern," by R. Langer, Ergebnisse der Aerodynamischen Versuchsanstalt zu Geottingen, IV Lieferung, 1932, pp. 138-141.

13 "Widerstand von Seidengazefilter, Runddraht - und Blech-streifensieben mit quadratischen Maschen," by O. Flachsbart, Ergebnisse der Aerodynamischen Versuchsanstalt zu Geottingen, IV Lieferung, 1932, pp. 112-118.

Captions for Illustrations

Fig. 1 Flow in a vee-gutter cascade

Fig. 2 Flow in a two-dimensional contraction

Fig. 3 Wake width parameter μ as a function of gutter half-angle α for various blockage b/t

Fig. 4 Wake width parameter μ as a function of blockage b/t for various gutter half-angle α

Fig. 5 Total pressure loss coefficient λ as a function of gutter half-angle α for various blockage b/t

Fig. 6 Total pressure-loss coefficient λ as a function of blockage b/t for various gutter half-angle α

Fig. 7 Drag coefficient C_D as a function of gutter half-angle α for various blockage b/t

Fig. 8 Drag coefficient C_D as a function of blockage b/t for various gutter half-angle α

Fig. 9 Sici spiral

Fig. 10 Flow in vee-gutter cascade of large gutter half-angle α and large blockage b/t

Fig. 11 Comparison of theory and experiment for single vee-gutter between parallel walls. Gutter half-angle α = 45 deg and various blockage b/t

Fig. 12(a) Spark Schlieren photograph of flow with combustion over single vee-gutter between parallel walls. Gutter half-angle α = 45 deg, blockage b/t = 0.75 and inlet velocity w_1 = 48.7 fps. Wake boundary calculated from loss measurements - - - theoretical wake boundary -·-·-

Fig. 12(b) Spark Schlieren photograph of flow without combustion over a single vee-gutter between parallel walls. Gutter half-angle $\alpha = 45$ deg, blockage $b/t = 0.75$ and inlet velocity $w_1 = 46.5$ fps. Wake boundary calculated from loss measurements - - - theoretical wake boundary -.-.-

Fig. 13 Comparison of theory and experiment for axisymmetric conical nozzles with various half-angle α and blockage b/t

Fig. 14 Comparison of theory and experiment for axisymmetric conical nozzles and flat plate cascades with half-angle $\alpha = 90$ deg and various blockage b/t

Fig. 15 Comparison of theory and experiment for cascades of gutter half-angle $\alpha = 90$ deg and various blockage b/t

Fig. 16 Comparison of theory and experiment for cascades of gutter half-angle $\alpha = 140.5$ deg and various blockage b/t

Fig. 17 Comparison of theory and experiment for cascades of gutter half-angle $\alpha = 180$ deg and various blockage b/t

Fig. 18 Comparison of theory and experiment for flow normal to sheet metal strip screens. Half-angle $\alpha = 90$ deg and various blockage b/t

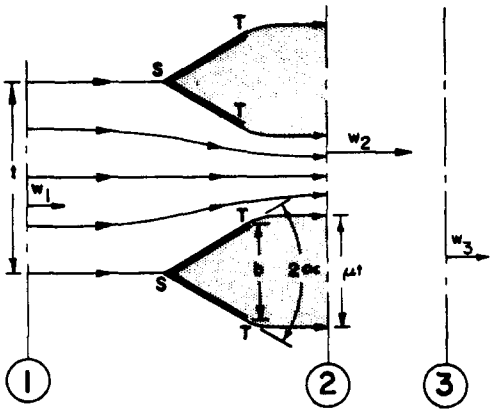

Fig.1

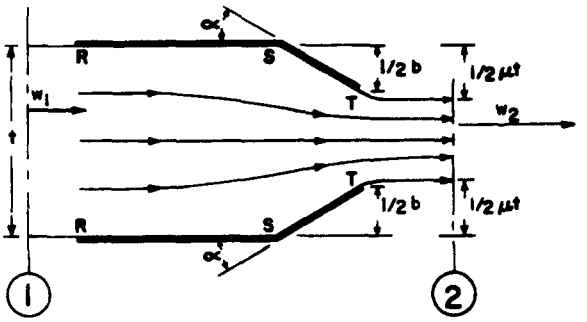

Fig.2

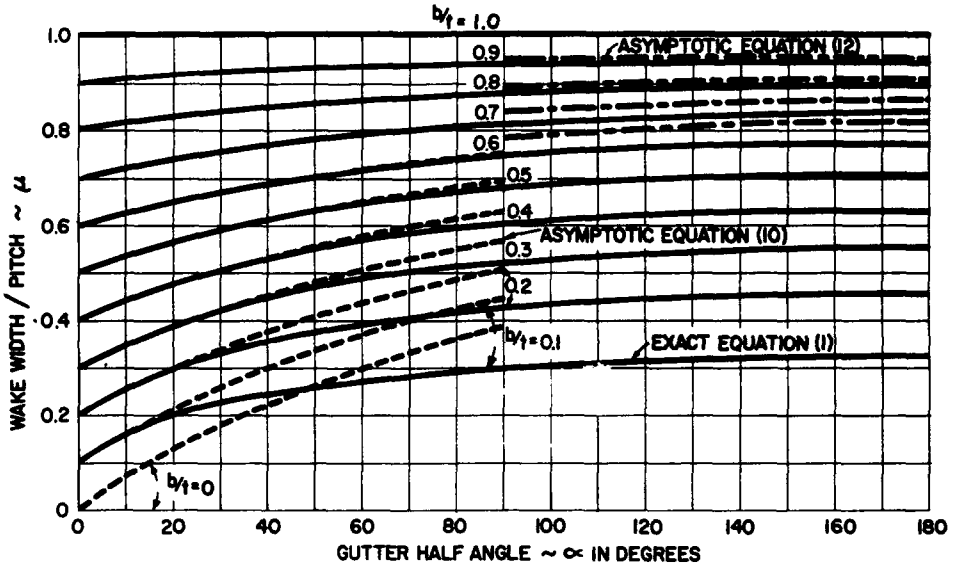

Fig.3

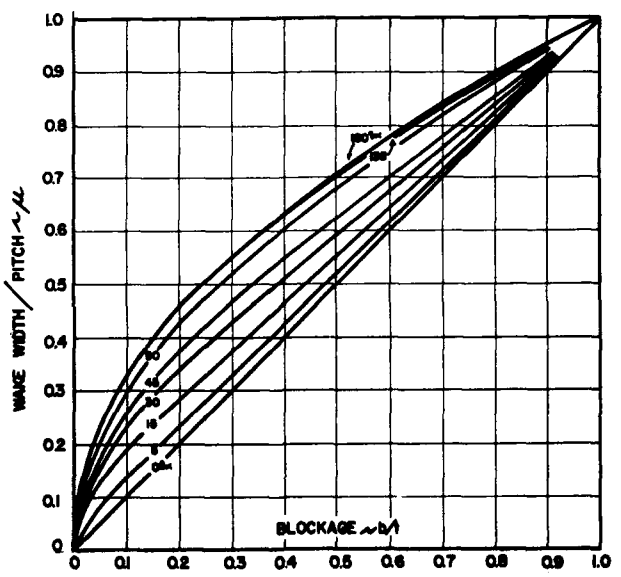

Fig.4

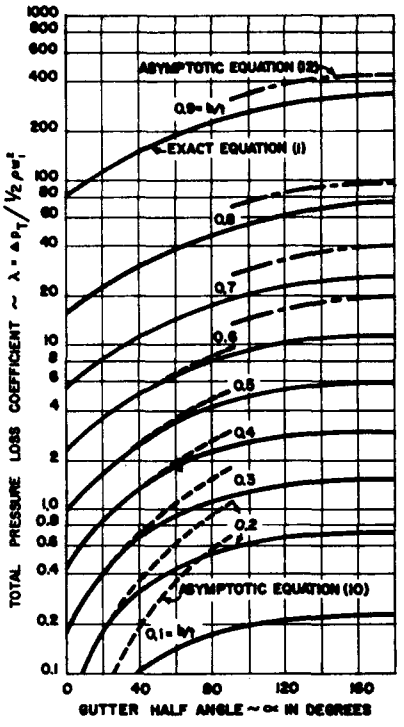

Fig.5

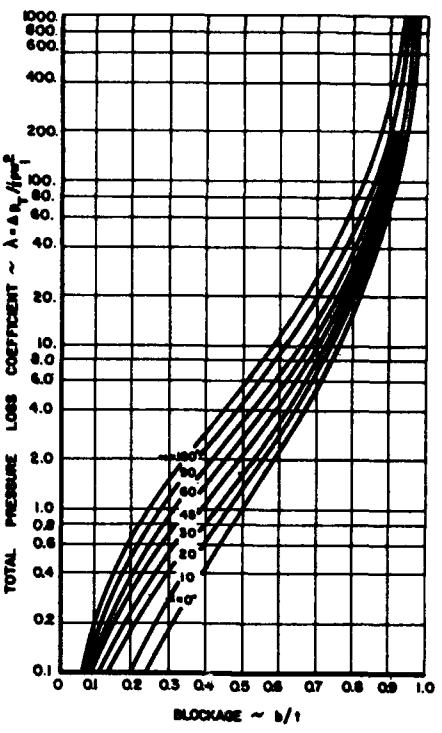

Fig.6

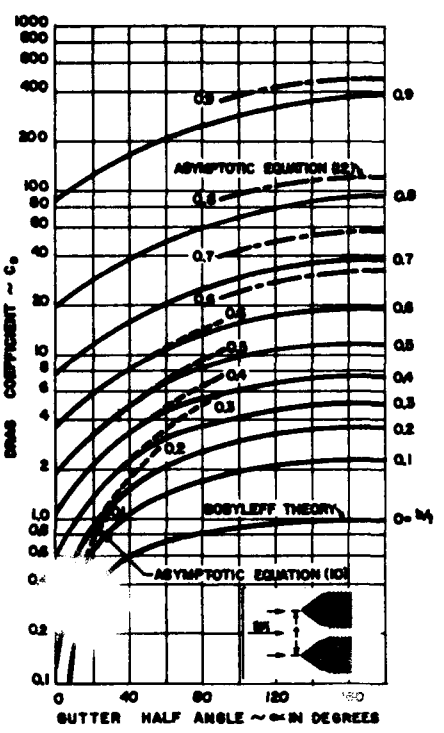

Fig.7

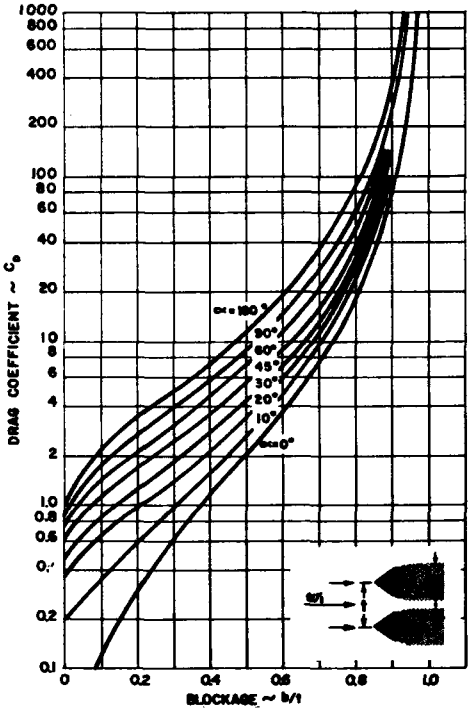

Fig.8

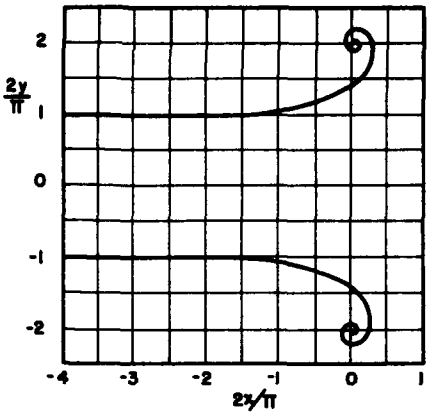

Fig.9

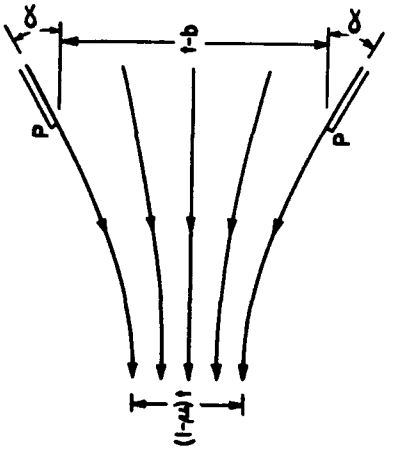

Fig.10

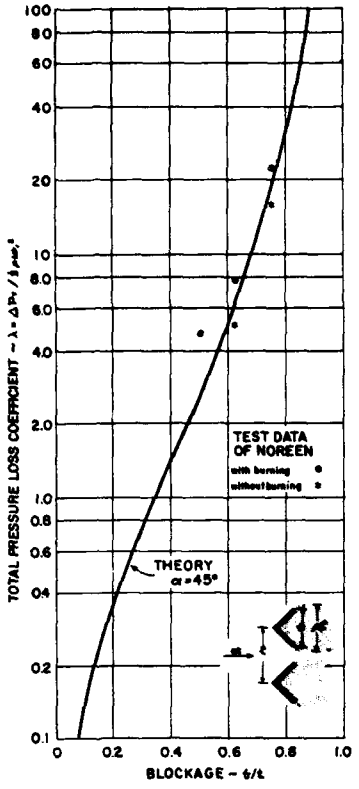

Fig.11

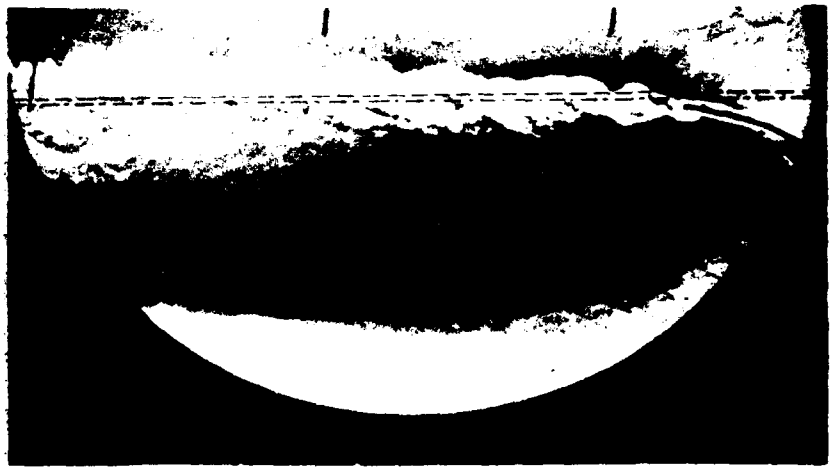

Fig.12(a)

Fig.12(b)

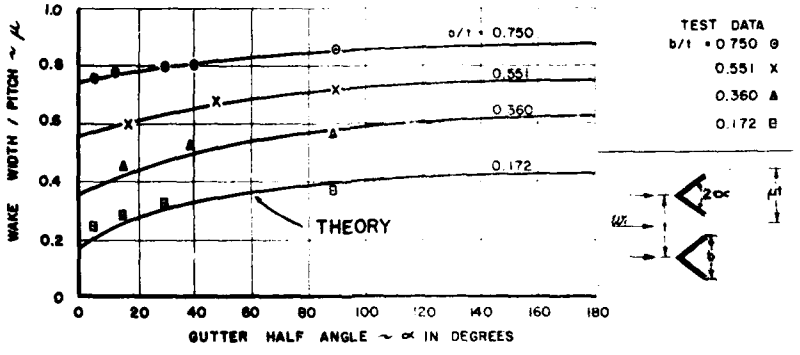

Fig.13

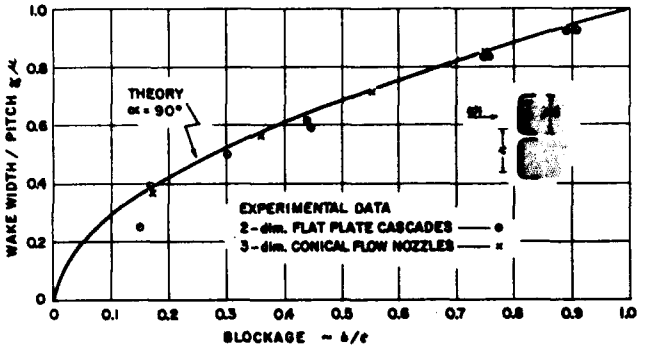

Fig.14

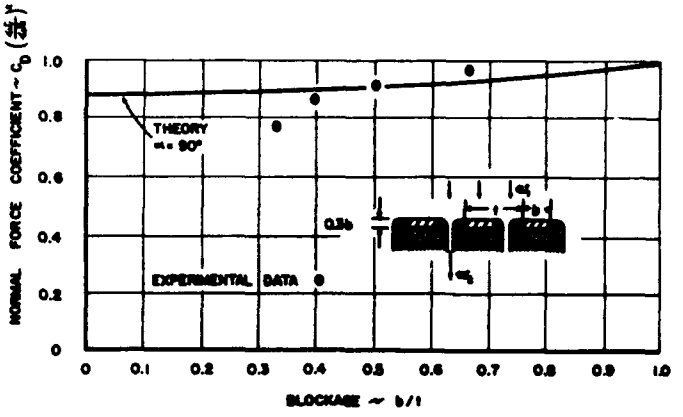

Fig.15

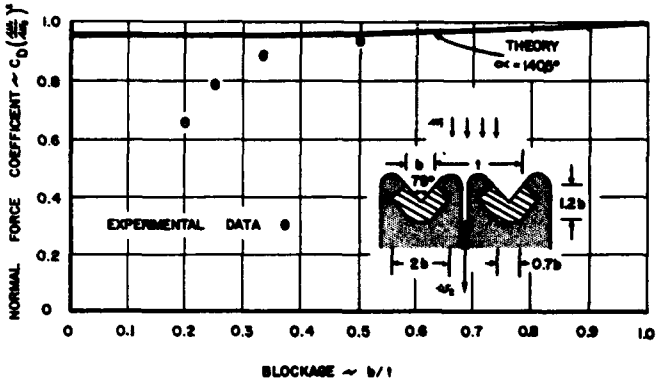

Fig.16

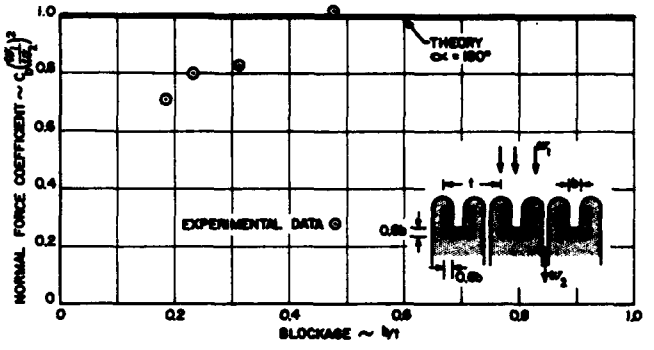

Fig.17

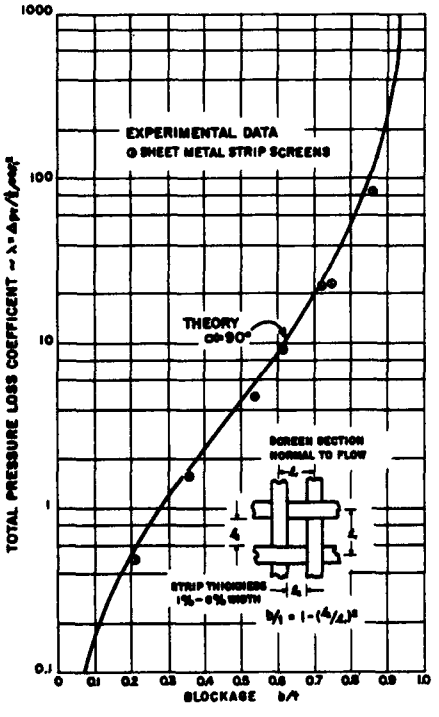

Fig.18